Evaluation of Rate Constants from Experimental Batch Reactor Data for Anionic Polymerization of Poly(methyl methacrylate) at High Temperatures

R. R. N. SAILAJA, ANIL KUMAR

Department of Chemical Engineering, Indian Institute of Technology, Kanpur 208016, India

Received 13 September 1996; accepted 30 December 1996

ABSTRACT: At high temperatures, in anionic polymerization, depolymerization and autocyclization reactions cannot be ignored and the molecular weight distribution (MWD) results based on irreversible polymerization give erroneous results. In this article, we have developed a semianalytical solution for the MWD of the polymer for a general complex mechanism. We then show that the various rate constants can be directly determined from the experimental data on MWD. After evaluating these, it is possible to model the anionic polymerization more rationally, as we have demonstrated using the experimental data from the literature. © 1997 John Wiley & Sons, Inc. J Appl Polym Sci **65:** 845–859, 1997

Key words: anionic polymerization; semianalytical; molecular weight distribution; living polymerization; cyclization; unequal reactivity; series solution technique

INTRODUCTION

Anionic polymerization is an important class of polymerization in which polymers having narrow molecular-weight distribution (MWD) and well-defined molecular structure (star, branched, block copolymers, etc.) can be found. Normally, the initiation step is extremely fast and chain growth occurs by the sequential addition of monomer to the growing centers. The propagation step of polymerization is affected by the gegen ion and the medium of the reaction mass. The experimental investigations[1–10] of "living polymerizing systems" have shown that different oligomers react with different rate constants. For extremely low temperatures (~ -46°C), anionic polymerization has been modeled as irreversible[7] and is represented by

$$P_n + M \xrightarrow{k_n} P_{n+1}; \quad n = 1, 2, \cdots \qquad (1)$$

It is common to assume that all rate constants are equal in value, and all results on the MWD derived in the literature assume this equal reactivity hypothesis. However, if polymerization occurs at higher temperatures (say at about 25°C), then depolymerization and autocyclization reactions cannot be ignored and the kinetic model can be represented by[11]

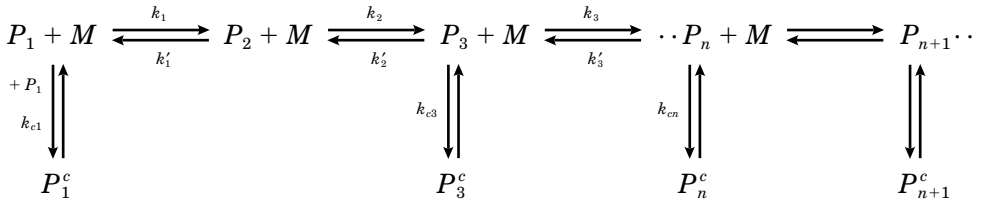

(2)

Correspondence to: A. Kumar.

 CCC 0021-8995/97/050845-15

Muller et al. have determined the MWD versus time of the poly(methyl methacrylate) formed by anionic polymerization and confirmed that k_1, k_2, and k_3 are substantially different. Through repeated numerical solution of the first three oligomers (P_1, P_2, and P_3) using a simplex method, they proposed the following model:

$$k_1 \neq k_2 \neq k_3$$
$$k_3 = k_4 = \cdots = k_p(\text{say}) \qquad (3)$$

With this kinetic model, we numerically solved the concentrations of higher oligomers, and on comparison with the reported experimental data on MWD versus time, we found a large deviation of as much as 1,000%. In view of the fact that the above rate constants yield only partial MWD, we wanted to reexamine this problem and in the following evolved a more systematic technique of determining rate constants for the experimental MWD versus time for anionic polymerization.

In this article, we have determined a semianalytical solution for the MWD of the polymer formed in anionic polymerization having a complex kinetic model in batch reactors in the monomer conversion domain. This way, the task of the numerical solution of ordinary differential equations (ODEs) (which could at times be unstable) is reduced to a sequential evaluation of algebraic functions which is shown to be inherently stable. We have applied these results to a set of experimental MWD and conversion data of polymerization from the literature to determine rate constants directly. After determining these, we have proposed a simplified kinetic model which gives an extremely good representation of anionic polymerization at higher temperatures.

MATHEMATICAL DEVELOPMENT

Solution of Anionic Polymerization in Conversion Domain

The equations governing the MWD of anionic polymerization represented by eq. (2) are sets of ODEs, summarized in Table I, which are nonlinear in nature. A study of these equations reveals that the MWD can be obtained only when $[M]$ and $[P_1]$ to $[P_{10}]$ are known beforehand. In order to determine a semianalytical solution of the MWD of Table I, we divide the conversion domain into smaller steps, as shown in Figure 1, and define u in the jth step such that

$$u = x - x_{j-1} \qquad (4)$$

We write the MWD of the polymer and the time of polymerization as an infinite series in u as follows:

$$t_j = t_{j-1} + \sum_{i=1}^{\infty} h_i u^i \qquad (5a)$$

$$[P_n] = [P_n]_{j-1} + [M]_{j-1} \sum_{i=1}^{\infty} \gamma_{ni} u^i \quad (n \geq 1) \qquad (5b)$$

To determine h_i and γ_{ni}, we substitute these in the set of ODEs and evaluate them through simple algebraic relations, as developed in Appendix I. This way, the solution of ODEs is reduced to determining the algebraic functions of eq. (5) sequentially. We have found that the semianalytical solution, eq. (5), is at least 20 times faster than Gear's algorithm. This is considerably easier to implement on any personal computer; it removes the stiffness of the ODEs governing the MWD and is extremely well suited to determine the rate constants, as we show below.

Evaluation of Rate Constants

The rate constants in the complex mechanism of anionic polymerization given in Table I are computed by use of the Box Complex search technique. Experimental data for eight different times have been reported, and we define the objective function as the cumulative error between the simulated and the experimental values of the various oligomer concentrations as

$$F = \left[\sum_{i=1}^{10} \sum_{j=1}^{8} \alpha_i' (P_{i,j}^e - P_{i,j}^c)^2 \right] \qquad (6)$$

Above, $P_{i,j}^e$ represents the experimental value of species P_i at times j. Muller et al.[11] reported experimental data for 10 species (i.e., $i_{\max} = 10$) for eight discrete times (i.e., $j_{\max} = 8$). The superscript e refers to the experimental data, while c denotes the computed concentration of the species P_i at the jth time. Various rate constants are varied using the algorithm of the Box Complex search and are summarized in the form of a flow chart (Fig. 2). The list of the weightage factors used for obtaining the values of the rate constants is given in Table II. The weightage factors are especially high for higher oligomers to compensate for their very low concentrations and hence improve the sensitivity of the objective function, F. The final

Table I ODEs Governing the MWD for Kinetic Model of Eq. (2)

MWD equations

$$\frac{d[P_1]}{dt} = -k_1[M][P_1] - k_1'[P_2] - 2k_{c1}[P_1]^2 \tag{T1.1}$$

$$\frac{d[P_2]}{dt} = k_1[M][P_1] + k_2'[P_3] - k_2[M][P_2] - k_1'[P_2] \tag{T1.2}$$

$$\frac{d[P_i]}{dt} = k_{i-1}[M][P_{i-1}] + k_i'[P_{i+1}] - k_i[M][P_i] - k_{i-1}'[P_i] - k_{ci}[P_i]. \qquad 3 \le i \le 9 \tag{T1.3}$$

$$\frac{d[P_n]}{dt} = k_p[M]([P_{n-1}] - [P_n]) + k_p'([P_{n+1}] - [P_n]) - k_c[P_n]\ n > 9 \tag{T1.4}$$

Monomer consumption

$$\frac{d[M]}{dt} = \sum_{i=1}^{9} k_i'[P_{i+1}] - \sum_{i=1}^{9} k_i[M][P_i] + k_p'\left(\lambda_0 - \sum_{n=1}^{10}[P_n]\right) - k_p[M]\left(\lambda_0 - \sum_{n=1}^{9}[P_n]\right) \tag{T1.5}$$

where,

$$\lambda_0 = \sum_{n=1}^{\infty}[P_n]$$

Cyclization products

$$\frac{d[P_1^c]}{dt} = k_{c1}[P_1]^2 \tag{T1.6}$$

$$\frac{d[P_n^c]}{dt} = k_{cn}[P_n] \qquad \text{for } n \ge 3 \tag{T1.7}$$

The initial conditions given by

$$\text{at } t = 0,\ [P_i] = [P_{i0}]$$

$$[P_i^c] = [P_{i0}^c] \tag{T1.8}$$

Generating function

We define a generating function, G, as follows

$$G = \sum_{n=1}^{\infty} s^n[P_n] \tag{T1.9}$$

where, s is a dummy variable less than unit.

$$\begin{aligned}\frac{dG}{dt} = {} & s(k_1'[P_2] - k_1[M][P_1] - 2k_{c1}[P_1]^2) + s^2(k_1[M][P_1] + k_2'[P_3] - k_2[M][P_2] - k_1'[P_2]) \\ & + \sum_{i=3}^{9}\{s^i k_{i-1}[M][P_{i-1}] + k_i'[P_{i+1}] - k_i[M][P_i] - k_{i-1}'[P_i] - k_{ci}[P_i]\} + s^{11}(k_9[M][P_9]) \\ & + (k_p[M]s^2 - k_p[M]s - k_c s)\left(G - \sum_{n=1}^{9} s^n[P_9]\right) + \left(G - \sum_{n=1}^{10} s^n[P_9]\right)(k_p' - k_p' s)\end{aligned} \tag{T1.10}$$

Above

$$k_{10} = k_{11} = \cdots = k_p \tag{T1.11}$$

values of rate constants give F of the order of 10^{-20} and are found to be independent of the arbitrary parameter α_i', which indicates that for these values of rate constants, the simulated results pass through all experimental points.

We have used 10 species (i.e., up to P_{10}) for our computation. We have chosen a total of 26 rate constants (equal to the number of experimental datum points) considering propagation, depropagation, and cyclization rate constants. The list of

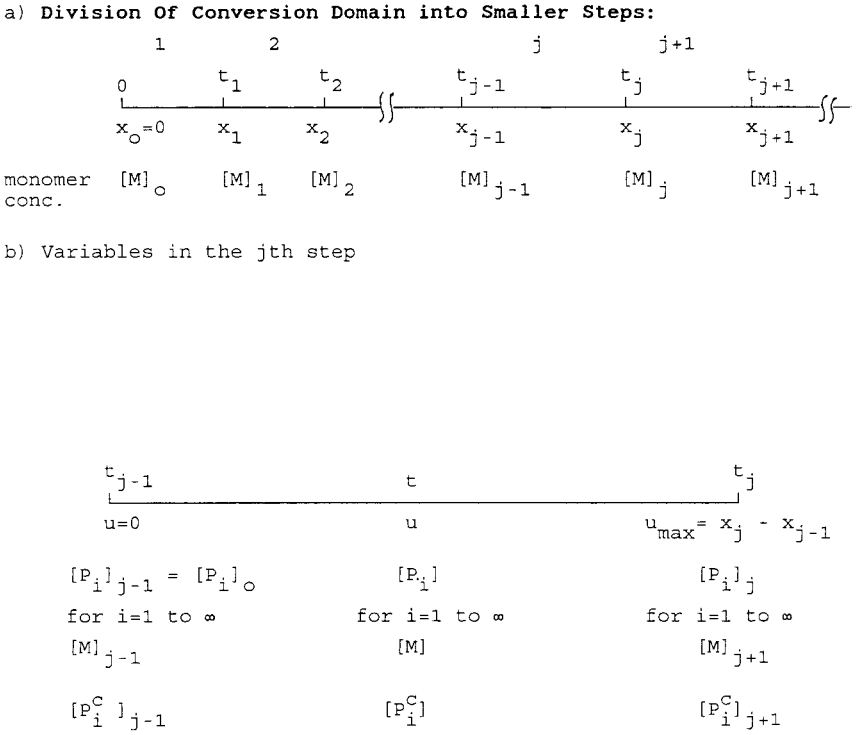

Figure 1 Division of step size for the semianalytical solution technique. conc., concentration.

upper (G_i') and lower (H_i) bounds of the different rate constants is given in Table III. Table IV gives different monomer concentrations for which studies have been made, and Table V gives a list of propagation, depropagation, and cyclization rate constants which describe the experimental data exactly. We observe a marked difference between k_1, k_2 and k_{c3}, and k_{c3} is quite high as compared with the other cyclization rate constants. This is because $[P_3^c]$ is the predominant cyclization product obtained with the progress of the reaction.

RESULTS AND DISCUSSION

Anionic polymerization of methyl methacrylate (MMA) at higher temperatures (say at 25°C) has been shown to consist of depolymerization and autocyclization steps, and the assumption of equal reactivity hypothesis breaks down, as shown in eq. (2). In this article, we have undertaken to analyze this problem in the conversion domain, and using the semianalytical solution given in Appendix I, we have determined the rate constants of the kinetic model directly from the batch experimental data.

Muller et al.[11] have carried out studies on the anionic polymerization of MMA at high temperature for three different monomer concentrations, as given in Table IV. They have determined the rate constants using the simplex method to curve fit their experimental data. Their analysis showed that the rate constants were dependent on the chain length of the oligomers, and they assumed that for chain length, n (≥ 3), the rate constants were independent of n. However, while carrying out numerical simulation using their rate constants, we found that the concentration of species $[P_4]$, $[P_5]$, etc., versus time was poorly represented and results often deviated by at least 1,000% from the experimental data. We proposed a more comprehensive model having unequal reactivity up to P_8 involving 26 rate constants (for 26 experimental points). We have already pointed out that our solution is semianalytical (in the sense that they are infinite series) in nature; as a result, rate constants reported by us are free of any possible numerical instability. Because there is no explicit relation between $[P_n]$ versus time and rate constants, the latter values are determined through repeated simulation. The variation of the set of rate constants between any two simulations was achieved by use of the Box Complex search technique. The total number of iterations to reach F having a value of 10^{-20} was about 33, and this F value was found to be independent

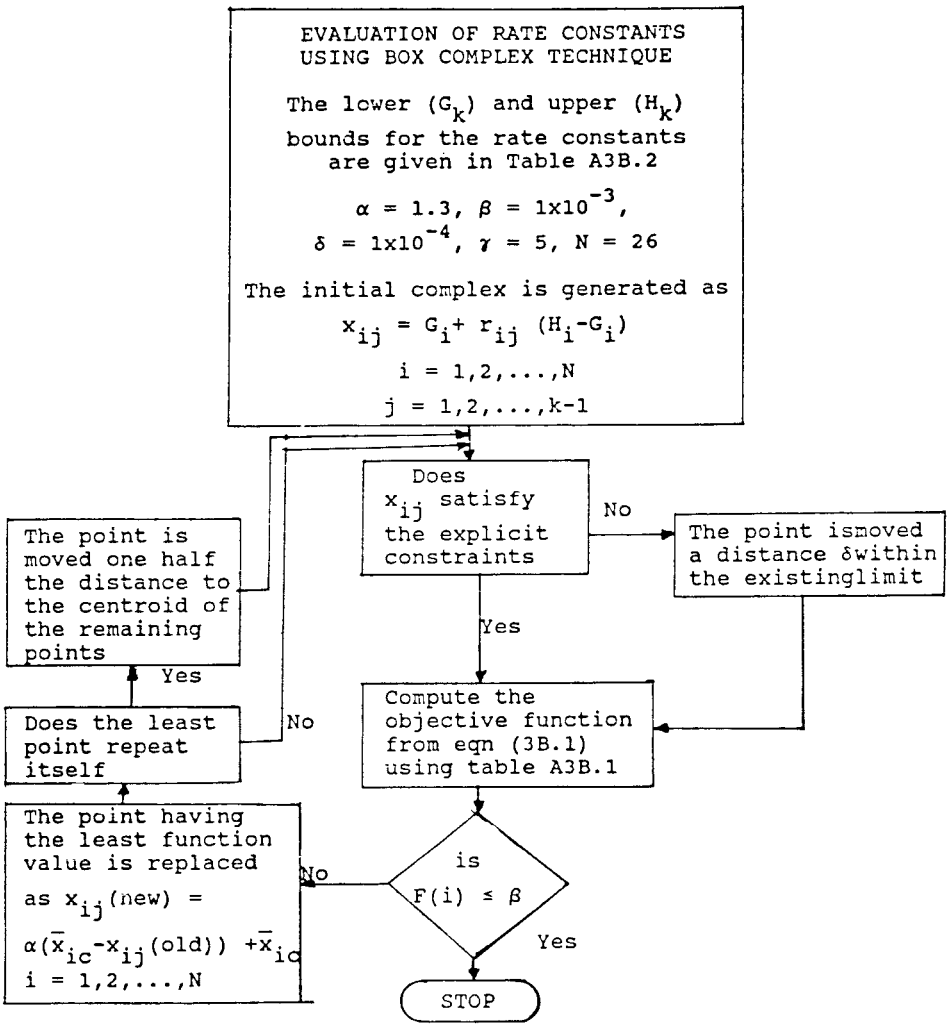

Figure 2 Flowchart for the Box Complex technique.

of choice of α_i' in eq. (6). This suggests that the experimental values lie on the simulation of $[P_n]$ versus t for any n, which we confirmed through simulation for these rate constants (given in Table V).

Figure 3 gives a plot of $\log(K_i)$ and $\log(k_i)$ versus chain length, i. In this figure, we observe a considerable difference between k_1 and k_2. Muller et al.[11] assumed $k_3 = k_4 = \cdots k_p$, but if we compare our results of Table V, we find a substantial difference. The association constants can be evaluated by use of the following expression:

$$k_i = \tfrac{1}{2}k_{iass} + (k_{i\pm} - \tfrac{1}{2}k_{iass}) \times [1/(2K_{iass}/\lambda_0)^{1/2}] \quad (7)$$

Above, k_{iass}, $k_{i\pm}$, K_{iass}, and λ_0 are, respectively, the rate constant for association for the ith oligomer, the rate constant for polymerization via ion pairs, the equilibrium constant for association, and the total concentration of the living oligomers. In our computations, we have assumed that the equilibrium constant for association is independent of chain length and is equal to 1,000 L mol^{-1} s^{-1}. Figure 4 shows a plot of $(1/\lambda_0)^{1/2}$ versus k_i. The list of association constants and the rate constants, $k_{i\pm}$, are given in Table VI. It is seen that the association constants keep increasing beyond the fifth oligomer and level off at 301.20 L mol^{-1} s^{-1} after

Table II List of Weightage Factors for the Rate Constants

i	α_i'
1	1
2	10
3	10
$i \geq 4$	100

Table III Upper and Lower Constraints for the Rate Constants in the Scheme Given in Eq. (5)

N	x_i	G_i'	H_i
1	k_1	4,000	5,000
2	k_2	50	220
3	k_3	150	200
4	k_4	120	215
5	k_5	120	230
6	k_6	120	220
7	k_7	120	220
8	k_8	120	220
9	k_1'	1×10^{-4}	5×10^{-4}
10	k_2'	0.1	0.3
11	k_3'	0.1	0.3
12	k_4'	0.1	0.3
13	k_5'	0.1	0.3
14	k_6'	0.1	0.3
15	k_7'	0.1	0.3
16	k_8'	0.1	0.3
17	k_{c1}	1×10^{-4}	5×10^{-4}
18	k_{c3}	20.0	30.0
19	k_{c4}	0.1	0.3
20	k_{c5}	0.1	0.3
21	k_{c6}	0.1	0.4
22	k_{c7}	0.1	0.3
23	k_{c8}	0.1	0.3
24	k_p	120	220
25	k_p'	0.1	0.4
26	k_c	0.1	0.4

P_6. $[P_2]$ has the largest rate constant for polymerization via ion pairs, followed by $[P_5]$. In all of the above computations, we have assumed $k_{iass}\lambda_0 \gg 1$.

The overall result given above suggests a trend in the rate constants, and we propose the following simplified model:

$$k_1 \neq k_2 \neq k_3 \neq k_4$$
$$k_5 = k_6$$
$$k_i = k_p \quad i \geq 7$$
$$k_{ci} = 0.0$$

Table IV List of Different Monomer Concentrations Studied Experimentally[11]

Case No.	$[P_1]_o$ (mol/L)	Monomer Concentration (mol/L)
1	0.05	0.10
2	0.10	0.20
3	0.20	0.40

Table V Rate Constants Obtained from the Box Complex Technique for Reversible Anionic Polymerization of MMA

$[P_1]_o = 5 \times 10^{-2}$ mol/L	$[M]_o = 10 \times 10^{-2}$ mol/L
$k_1 = 4{,}796.39$	
$k_2 = 180.00$	
$k_3 = 170.00$	
$k_4 = 60.00$	
$k_5 = 176.90$	
$k_6 = 181.78$	
$k_7 = 190.89$	
$k_8 = 195.64$	
$k_1' = 2.29 \times 10^{-4}$	
$k_2' = 0.2225$	
$k_3' = 0.28$	
$k_4' = 0.23$	
$k_5' = 0.25$	
$k_6' = 0.29$	
$k_7' = 0.16$	
$k_8' = 0.17$	
$k_{c1} = 1.12 \times 10^{-4}$	
$k_{c3} = 22.19$	
$k_{c4} = 0.26$	
$k_{c5} = 0.28$	
$k_{c6} = 0.30$	
$k_{c7} = 0.29$	
$k_p = 215.44$	
$k_p' = 0.25$	$k_c = 0.29$

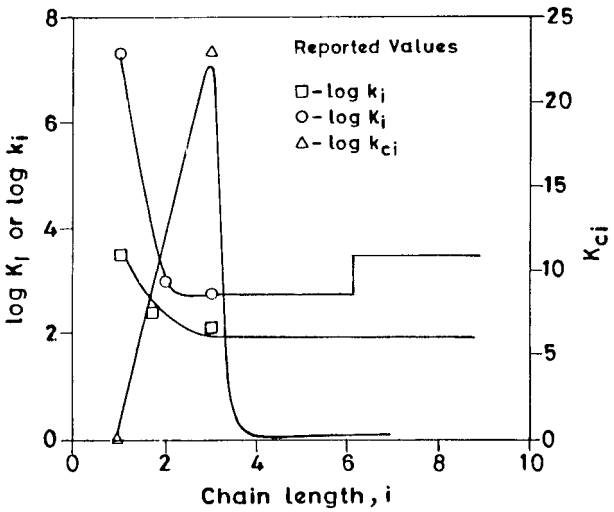

Figure 3 Chain length dependence of the rate equilibrium propagation and cyclization rate constants in the propagation of the reversible anionic polymerization of MMA.

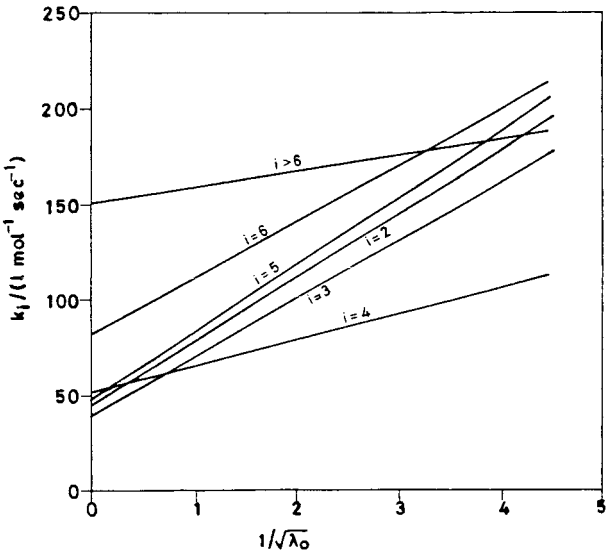

Figure 4 Plot of $1\sqrt{\lambda_0}$ versus k_i for the determination of association constants.

$$k_{ci} = k_c \quad i \geq 2$$

$$k_1' = 0.0$$

$$k_i' = k_p' \quad i \geq 2$$

The values of these rate constants are given in Table VII. We have simulated the MWD using the differential equation of Table I and then compared this simulated result with the experimental data.

Figures 5 and 6 show the comparison of the experimental results of Muller et al.[11] and those obtained by the semianalytical solution technique for the first six oligomers for case 1 (Table IV). Figure 6 also shows a plot of monomer conversion versus time for case 1. Similar computations were carried out for cases 2 and 3. Figures 7 and 8 show the plots for the first three oligomers in cases 2 and 3, respectively. The results of our technique have been found to match very well with the experimental results in the entire domain. It can be

Table VI List of Association Constants for the Reversible Anionic Polymerization of MMA

i	k_{iass} (L mol^{-1} s^{-1})	$k_{i\pm}$ (L mol^{-1} s^{-1})
2	92.72	1,371.57
3	81.85	1,037.67
4	103.43	501.17
5	95.32	1,125.66
6	177.77	991.33
($i \geq 6$)	301.20	557.89

Table VII List of the Rate Constants for the Proposed Model

$k_1 = 4{,}796.38$
$k_2 = 150.00$
$k_3 = 170.00$
$k_4 = 60.00$
$k_5 = 179.30$
$k_6 = 179.30$
$k_i = k_p = 215.44$ ($i > 6$)
$k_1' = 0.00$
$k_i' = k_p' = 0.257$ ($i > 2$); $k_{ci} = 0.00$; $k_{ci} = k_c = 0.27$ $i \geq 2$

seen that initiator (α-lithioisobutyrate), represented as $[P_1]$, completely disappears in 0.02 sec. $[P_2]$ and $[P_3]$ increase very quickly, reach a maximum, and decrease before leveling off at higher conversions. The concentrations of higher oligomers keep increasing and level off at slightly lower values. The concentrations of the cyclization products $[P_3^c]$ and $[P_4^c]$ are also plotted for each case. It can be seen that $[P_3^c]$ is the only major cyclization product. This increases with conversion before attaining a steady value at higher conversions. We have proceeded similarly for cases 2 and 3 (Table IV). It can be seen that higher initial monomer concentrations lead to fast and high conversions. Further, in cases 2 and 3, P_3 is completely consumed, while this is not so in case 1. The concentrations of $[P_4]$, $[P_5]$, and $[P_6]$ also

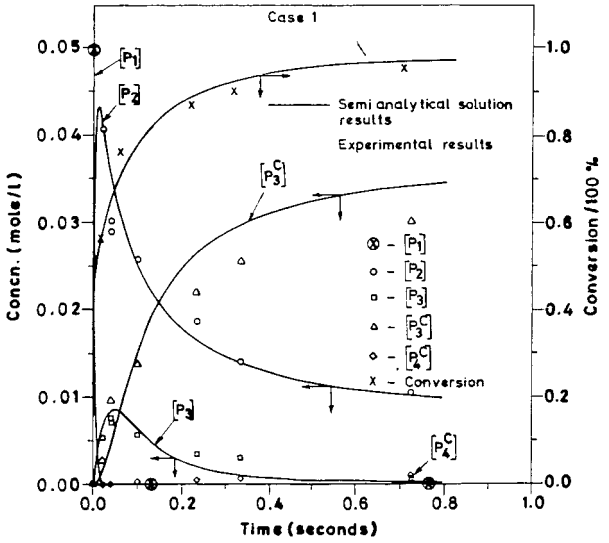

Figure 5 Comparison of simulated results with the experimental data of Muller et al.[11] for the first three oligomers for a monomer concentration (Concn.) of 0.1 mol/L (case 1).

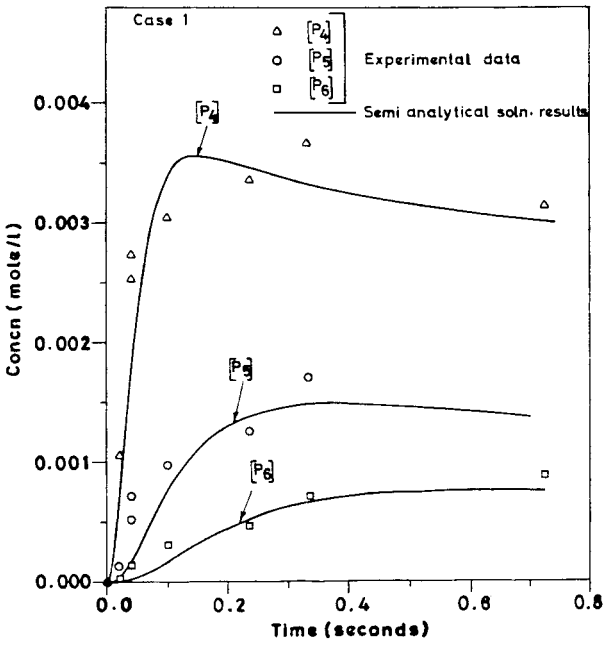

Figure 6 Comparison of simulated results with the experimental data of Muller et al.[11] for $[P_4]$, $[P_5]$, and $[P_6]$ for a monomer concentration (Concn) of 0.1 mol/L (case 1). soln., solution.

level off at higher values with increasing initial concentrations of the monomer.

CONCLUSIONS

In this article, we have developed a semianalytical solution of anionic polymerization with depolymerization and cyclization steps. Using the reported experimental data in the literature on the MWD of the polymer formed in the batch reactors, we have evaluated the rate constants. We have varied the rate constants between iterations using the Box Complex technique and minimized the mean square error between experimental and simulated MWD data to determine the chain length–dependent rate constants. At the optimal level, the total error F was reduced to a value of 10^{-20}, which was formed to be independent of the choice of weighting factors α_j. This result suggests that the simulated MWD passes through all of the experimental datum points. On the basis of the rate constants so determined, we have proposed a simplified kinetic model which describes the experimental observation very well.

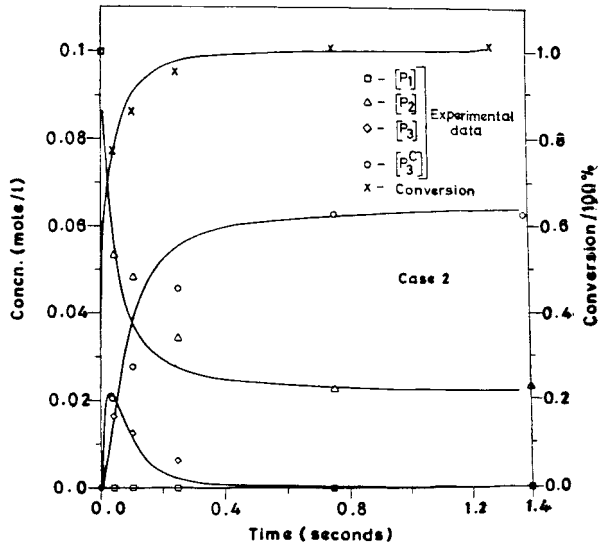

Figure 7 Comparison of simulated results with the experimental data of Muller et al. for the first three oligomers for a monomer concentration (Concn.) of 0.2 mol/L (case 2).

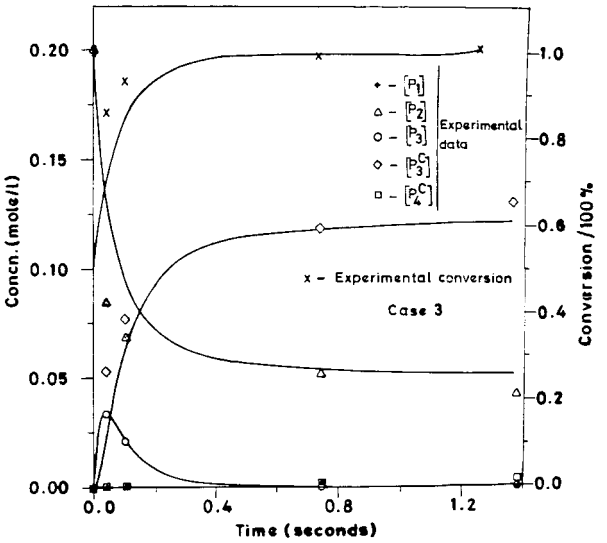

Figure 8 Comparison of simulated results with the experimental data of Muller et al. for the first three oligomer for a monomer concentration (Concn.) of 0.4 mol/L (case 3).

APPENDIX I. DERIVATION OF COEFFICIENTS FOR ANIONIC POLYMERIZATION OF MMA WITH AUTOCYCLIZATION AND DEPOLYMERIZATION

The equations governing the MWD of anionic polymerization are summarized in Table I. A study of equations in this table reveals that the MWD of the polymer formed can be obtained only when $[M]$ and $[P_1]$ to $[P_{10}]$ are known. In order to determine the h_i and γ_{ni} of eq. (4), we substitute these

equations into the differential equation for the moment generating function G as

$$\frac{sdG}{dt} = s^2[k_1'[P_2] - k_1[M][P_1] - 2k_{c1}[P_1]^2] + s^3[k_1[M][P_2] + k_2'[P_3 - k_2[M][P_2] - k_1'[P_2]] + \sum_{i=3}^{9} s^{i+1}(k_{i-1}[M][P_{i-1}] + k_1'[P_{i+1}] - k_i[M][P_i] - k_{i-1}'[P_i] - k_{ci}[P_i]) + s^{11}(k_9[M][P_9] - k_9'[P_{10}]) + (k_p[M]s^2 - k_p[M]s - k_c s) \quad \text{(I.1)}$$

We now assume a series for G as follows,

$$G = G_{j-1} + [M]_{j-1} \sum_{1}^{\infty} g_i u^i \quad \text{(I.2a)}$$

where

$$G_{j-1} = \sum_{1}^{\infty} s^n [P_{n,j-1}]. \quad \text{(I.2b)}$$

Substituting eq. (I.2) into eq. (I.1), we get

$$\frac{sdG}{dt} = s^2 \sum_{i=0}^{\infty} \alpha_i u^i + s^3 \sum_{i=0}^{\infty} \beta_i u^i + \sum_{n=3}^{9} s^{n+1}\theta_{n,i} + s^{11} \sum_{0}^{\infty} \delta_i u^i + (k_p[M]s^2 - k_p[M]s - k_c s) \times \left(G - \sum_{n=1}^{9} s^n[P_n]\right) + (k_p - k_p' s) \times \left(G - \sum_{n=1}^{10} s^n[P_n]\right) \quad \text{(I.3)}$$

where the coefficients α_i, β_i, $\theta_{n,i}$, δ_i are given in Table VIII. Eq. (I.3) can be written as

$$\frac{sdG}{dt} = \sum_{0}^{\infty} B_i u^i \quad \text{(I.4c)}$$

The coefficients B_i are given in Table IX. Now, each of the B_i' values can be written as series of s, and these are written as

$$B_i = \sum_{j=1}^{\infty} B_{ij} s^j \quad \text{(I.5)}$$

At any time t, the amount of monomer is related to the conversion, by the following relation:

Table VIII List of Coefficients for Eq. (I.3)

i	α_i	β_i	$\theta_{n,i}$ $(3 \le n \le 9)$	δ_i
0	$(k_1'[P_2]_0 - k_1[M]_0[P_1]_0 - 2k_{c1}[P_1]_0^2$	$k_1[M]_0[P_1]_0 + k_2'[P_3]_0 - k_2[M]_0[P_2]_0$	$k_{n-1}[M]_0[P_{n-1}]_0 k_n'[P_{n+1}]_0 - k_n[M]_0[P_n]_0$ $- k_{n-1}'[P_n]_0 - k_{cn}[P_n]_0)$	$(k_9[M_0[P_9]_0 - k_9'[P_{10}]_0)$
1	$(k_1'[M]_0\gamma_{2,1} - k_1[M]_0^2\gamma_{11} + k_1[M]_0[P_1]_0$ $- 4k_{c1}[P_1]_0[M]_0\gamma_{11}$	$(k_1[M]_0^2\gamma_{11} - k_1[M]_0[P_1]_0$ $+ k_2'[M]_0\gamma_{31} - k_2[M]_0^2\gamma_{21}$ $+ k_2[M]_0[P_2]_0$	$\{(k_{n-1}[M]_0([M]_0\gamma_{n-1,1} - [P_{n-1}]_0)$ $+ k_n'[M]_0(\gamma_{n+1,1}) - k_n[M]_0([M]_0\gamma_{n,1}$ $- [P_n]_0) - k_{n-1}'\gamma_{n,1}[M]_0$ $- k_{cn}\gamma_{n1}[M]_{01}\}$	$(k_9[M]_0^2\gamma_{9,1} - k_9[M_0[P_9]_0$ $- k_9'[M]_0\gamma_{10,1}$
i $(i \ge 2)$	$(k_1'[M]_0\gamma_{2,i} + k_1[M]_0^2(\gamma_{1,i-1} - \gamma_{1,i})$ $- 2k_{c1}(2[P_1]_0[M]_0\gamma_{1,i}$ $+ [M]_0^2 \sum_{j=1}^{i-1} \gamma_{1,j}\gamma_{1,i-j})$	$(k_1[M]_0^2(\gamma_{1,i} - \gamma_{1,i-1}) + k_2'[M]_0\gamma_{3,i}$ $- k_2[M]_0^2(\gamma_{2,i} - \gamma_{2,i-1})$	$\{(k_{n-1}[M]_0^2(\gamma_{n-1,i} - \gamma_{n-1,i-1})$ $+ k_n'[M]_0\gamma_{n+1,i} - k_n[M]_0^2(\gamma_{n,i}$ $- \gamma_{n,i-1}) - k_{n-1}'[M]_0\gamma_{n,i}$ $- k_{cn}[M]_0\gamma_{n,i}$	$k_9[M]_0^2(\gamma_{9,i} - \gamma_{9,i-1})$ $- k_9'[M]_0\gamma_{10,i}$

Note: subscript 0 represents concentrations of the species at the $(j-1)$th step.

Table IX List of Coefficients for Eq. (I.4)

i	B_i
0	$s^2\alpha_0 + s^3\beta_0 + \sum_{n=3}^{9} s^{n+1}\theta_{n,0} + s^{11}\delta_0 + k_p[M]_0 \sum_{1}^{\infty} s^{n+2}[P_n]_0 - (k_p[M]_0 + k_c) \sum_{1}^{\infty} s^{n+1}[P_n]_0$ $- k_p[M]_0 \sum_{1}^{9} s^{n+2}[P_n]_0 + (k_p[M]_0 + k_c) \sum_{1}^{9} s^{n+1}[P_n]_0 + (k'_p - k'_p s)\left(G_0 - \sum_{n=1}^{10} s^n[P_n]_0\right)$
1	$s^2\alpha_1 + s^3\beta_1 + \sum_{n3}^{9} s^{n+1}\theta_{n,1} + s^{11}\delta_1 - k_p[M]_0 \sum_{1}^{\infty} s^{n+1}[P_n]_0 + k_p[M]_0 \sum_{1}^{\infty} s^{n+1}[P_n]_0 + k_p[M]_0^2 s g_1(s-1)$ $- k_c[M]_0 g_1 s - k_p[M]_0^2 \sum_{1}^{9} s^{n+2}\gamma_{n,1} + (k_p[M]_0 \sum_{1}^{9} s^{n+2}[P_n]_0 + (k_p[M]_0^2 + k_c[M]_0) \sum_{1}^{9} s^{n+1}\gamma_{n,1}$ $- (k_p[M]_0 \sum_{1}^{9} s^{n+1}[P_n]_0 + [M]_0(k'_p - k'_p s)\left(g_1 - \sum_{2}^{10} s^n\gamma_{n,1}\right)$
i ($i \geq 2$)	$s^2\alpha_i + s^3\beta_i + \sum_{n=3}^{9} s^{n+1}\theta_{n,i} + s^{11}\delta_i + (g_i - g_{i-1})(k_p[M]_0^2 s^2 - k_p[M]_0^2 s) - k_c[M]_0 s g_i - k_p[M]_0^2 \sum_{1}^{9} s^{n=2}$ $\times (\gamma_{n,1} - \gamma_{n,i-1}) + k_p[M]_0^2 \sum_{n=1}^{9} s^{n+1}(\gamma_{n,i} - \gamma_{,i-1}) + k_c[M]_0) \sum_{n=1}^{9} s^{n+1}\gamma_{n,i} + (k'_p[M]_0\left(g_i - \sum_{1}^{10^1} s^n\gamma_{n,i}\right)$ $- k'_p[M]_0\left(g_i s - \sum_{1}^{10} s^{n+1}\gamma_{n,i-1}\right)$

Note: subscript 0 stands for concentrations of species at the $(j-1)$th step.

$$[M] = [M_{j-1}](1-u) \tag{I.6}$$

Substituting eq. (I.6) into eq. (T1.4) of Table I, we obtain the rate of change in monomer conversion as follows:

$$\frac{du}{dt} = \sum_{i=0}^{\infty} A_i u^i \tag{I.7}$$

where

$$A_0 = -\frac{1}{[M_{j-1}]}\left[\sum_{n=1}^{\infty}(k'_n[P_{n+1,j-1}] - k_n[M_{j-1}][P_{n,j-1}])\right]$$

$$A_1 = -\frac{1}{[M_{j-1}]}\left[\sum_{n=1}^{\infty}(k'_n[M_{j-1}]\gamma_{n+1,1} - k_n[M_{j-1}]([M_{j-1}]\gamma_{n,1} - [P_{n,j-1}]\right]$$

$$A_i = -\frac{1}{[M_{j-1}]}\left[\sum_{n=1}^{\infty}(k'_n[M_{j-1}]\gamma_{n+1,i} - \mathrm{k}_n[M_{j-1}](\gamma_{n,i} - \gamma_{n,i-1})\right] \text{ for } i \geq 2 \tag{I.8c}$$

$$\int_{t_{j-1}}^{t_j} dt = \int_{u_{j-1}}^{u_j}\left(\frac{1}{\sum_{i=0}^{\infty} A_i u^i}\right) \tag{I.9}$$

Now

$$\left(\frac{1}{\sum_{i=0}^{\infty} A_i u^i}\right) = \sum_{i=0}^{\infty} y_i u^i \tag{I.10}$$

where

$$y_0 = \frac{1}{A} \tag{I.11a}$$

$$y_1 = -\frac{y_0 A_1}{A_0} \tag{I.11b}$$

$$y_i = -\sum_{k=1}^{i-1} y_{i-k}A_k \quad \text{for } i \geq 2 \tag{I.11c}$$

$$\Delta t = \sum_{i=1}^{\infty} h_i u^i \tag{I.11d}$$

Above,

$$h_i = \frac{y_{i-1}}{i} \quad \text{for } i = 1, 2, 3, \cdots \tag{I.12}$$

Above, we have assumed $k_{10} = k_{11} = \cdots = k_p$ The lefthand side of eq. I.1 can be written as

$$\frac{sdG}{du}\frac{du}{dt} = s\sum_{1}^{\infty} i g_i u^{i-1} \sum_{0}^{\infty} A_i u^i \tag{I.13a}$$

$$= s\sum_{0}^{\infty} D_i u^i \tag{I.13b}$$

where,

$$D_0 = g_1 A_0 \qquad \text{(I.13c)}$$

$$D_1 = g_1 A_1 + 2g_2 A_0 \qquad \text{(I.13d)}$$

$$D_i = \sum_{j=1}^{i+1} j g_j A_{i-j} \quad \text{for } i \geq 2 \qquad \text{(I.13e)}$$

Hence, eqs. (I.5) and (I.13) can be incorporated into eq. (I.2) to get

$$sM_0 \sum_0^\infty D_i u^i = \sum_{i=0}^\infty u^i \sum_{j=2}^\infty B_{ij} s^j \qquad \text{(I.14)}$$

In the above equation, we have not considered B_{i1}. We have seen in Table X that B_{i1} is essentially equal to zero for all values of i. Hence, equating equal powers of u on both sides of eq. (I.14), we get, for $i = 0$

$$s[M]_0 D_0 = \sum_{j=2}^\infty B_{0j} s^j \qquad \text{(I.15a)}$$

or

$$g_1 A_0 [M]_0 = \sum_{j=2}^\infty B_{0j} s^{j-1} \qquad \text{(I.15b)}$$

or

$$g_1 = \frac{1}{A_0[M]_0} \sum_{j=2}^\infty B_{0j} s^{j-1} \qquad \text{(I.15c)}$$

or

$$g_1 = \sum_{k=1}^\infty g_{1k} s^j \qquad \text{(I.15d)}$$

where,

$$g_{1k} = \frac{B_{0,k+1}}{A_0[M_{j-1}]} \quad j = 1, 2, 3, \cdots \qquad \text{(I.15e)}$$

In general, for any value of i we can write

$$g_i = \sum_{j=1}^\infty g_{ij} s^j \qquad \text{(I.16a)}$$

where,

$$g_{ij} = \frac{1}{iA_0}\left[\frac{B_{i-1,j+1}}{[M_{j-1}]} - \sum_{k=1}^{i-1} k g_{k,j} A_{i-k}\right] \qquad \text{(I.16b)}$$

Table X Coefficients Appearing in Eq. I.14 of Appendix I

i	B_{i1}	B_{i2}	B_{i3}	B_{i4}	B_{i5}	B_{i6}	B_{i7}	B_{i8}	B_{i9}	B_{i10}	B_{i11}	B_{ik} $(k \geq 12)$
0	0	α_0	β_0	θ_{30}	θ_{40}	θ_{50}	θ_{60}	θ_{70}	θ_{80}	θ_{90}	$\delta_0 - k_c[P_{10}]_0 + k'_p([P_{11}]_0 - [P_{10}]_0)$	$k_p[M]_0([P_{k-2}]_0 - [P_{k-1}]_0) - k_c[P_{k-1}]_0 + k'_p([P_{k-2}]_0 - [P_{k-1}]_0 - [P_{k-2}]_0)$
1	0	α_1	β_1	θ_{31}	θ_{41}	θ_{51}	θ_{61}	θ_{71}	θ_{81}	θ_{91}	$\delta_1 + k'_p[M]_0 g_{1,11} - k_c[M]_0 g_{1,10}$	$k_p[M]_0([P_{k-1}]_0 - [P_{k-2}]_0) + k_p[M]_0^2(g_{1,k-2} - g_{1,k-1}) - k_c[M]_0 g_{1,k-1} + k'_p[M]_0 \times (g_{1,k} - g_{1,k-1})$
$i \geq 2$	0	α_i	β_i	θ_{3i}	θ_{4i}	θ_{5i}	θ_{6i}	θ_{7i}	θ_{8i}	θ_{9i}	$\delta_i + k_p[M]_0^2(g_{i-1,10} - g_{i,10}) - k_c[M]_0 g_{i,10} + k'_p[M]_0(g_{i,11} - g_{i-1,11})$	$k_p[M]_0^2(g_{i,k-2} - g_{i-1,k-2}) + k_p[M]_0^2 \times (g_{i-1,k-1} - g_{i,k-1}) - k_c[M]_0 g_{i,k-1} + k'_p[M]_0(g_{i,k} - g_{i-1,k-1})$

Note: subscript 0 stands for concentration of species at the $(j-1)$th step.

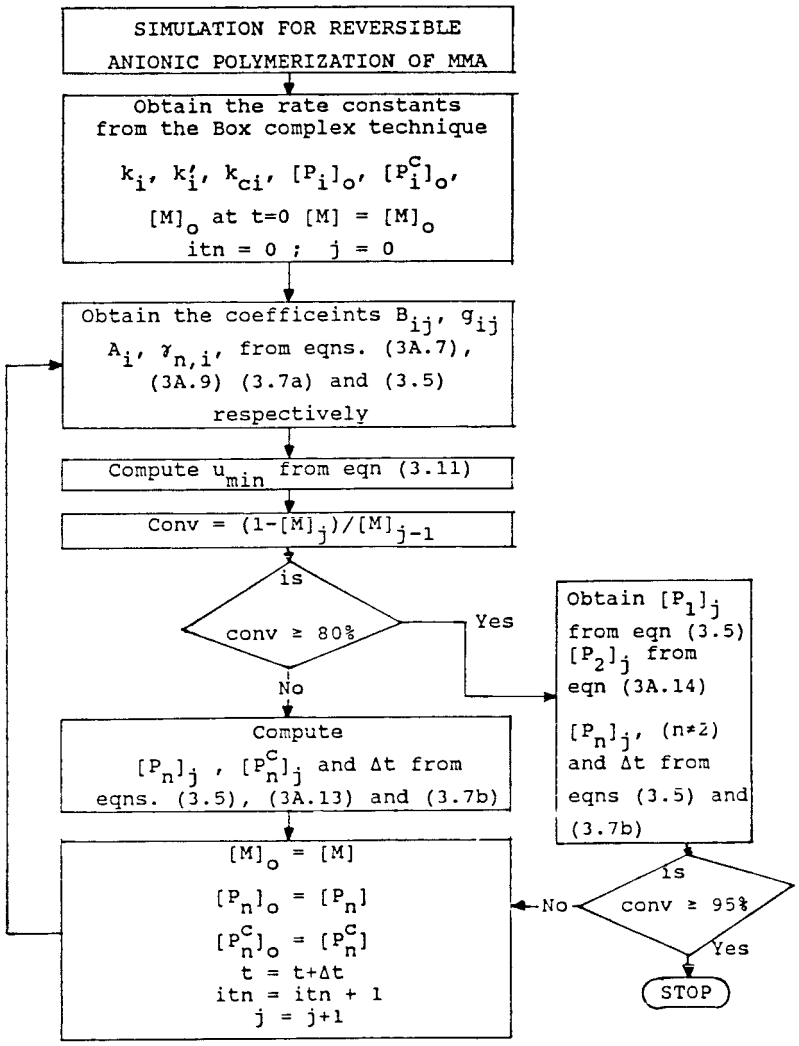

Figure 9 Flowchart for the determination of MWD for the reversible anionic polymerization of MMA.

Table XI Coefficients for the Cyclization Products [Eq. (I.20)

i	$a1_i$	$c1n_i$ $(n \geq 3)$
1	$k_{c1}[P_1]_0^2/([M]_0A_0)$	$k_{cn}[P_n]_0/(A_0[M]_0)$
2	$(1/(2A_0))(2[P_1]_0g_{11}k_{c1} - a1_1A_1)$	$(1/(2A_0))(k_{cn}g_{1n} - c1n_1A_1)$
i $(i \geq 3)$	$(1/(iA_0))(2[P_1]_0k_{c1}g_{i-1,1} + [M]_0k_{c1}\sum_{j=1}^{i-2} g_{j1}g_{i-j-1,1} - \sum_{j=1}^{i-1} ja1_jA_{i-j})$	$(1/(iA_0))(k_{cn}g_{i-1,n} - \sum_{j=1}^{i-1} jc1n_jA_{i-j})$

Note: subscript 0 stands for concentration of species at $(j-1)$th step.

Table XII Effect of Number of Terms on Oligomer Concentration at 70% Conversion

No. of Terms	$[P_1]$	$[P_2]$	$[P_3]$	$[P_4]$	$[P_5]$	$[M]$	t (s)
1	0.0489×10^{-7}	0.0316	0.0086	0.0019	0.2196×10^{-3}	0.0291	0.0537
2	0.2069×10^{-5}	0.0317	0.0084	0.0019	0.2515×10^{-3}	0.0291	0.0551
3	0.5059×10^{-6}	0.0317	0.0083	0.0019	0.2544×10^{-3}	0.0291	0.0553
4	0.6404×10^{-6}	0.0317	0.0083	0.0019	0.2546×10^{-3}	0.0291	0.0553
5	0.6252×10^{-6}	0.0317	0.0083	0.0019	0.2546×10^{-3}	0.0291	0.0553
10	0.6252×10^{-6}	0.0317	0.0083	0.0019	0.2546×10^{-3}	0.0291	0.0553
RK	0.6353×10^{-6}	0.0314	0.0083	0.0019	0.2548×10^{-3}	0.0291	0.0553

Initial concentrations are $[M]_0 = 0.1$; $[P_1]_0 = 0.05$. All concentrations are in moles per liter.

Hence, expanding eq. (I.3a), we get

$$\sum s^n[P_n] = \sum s^n[P_{n,j-1}] + [M_{j-1}] \sum_{j=1}^{\infty} u^i \sum_{k=1}^{\infty} g_{ij} s^j \quad \text{(I.17)}$$

Equating equal powers of s on both sides of eq. (I.17), we get the concentration of any species n as

$$[P_n] = [P_n]_{j-1} + [M]_{j-1} \sum_{i=1}^{\infty} g_{in} u^i \quad \text{(I.18)}$$

The list of coefficients for B_{ij} is given in Table X.

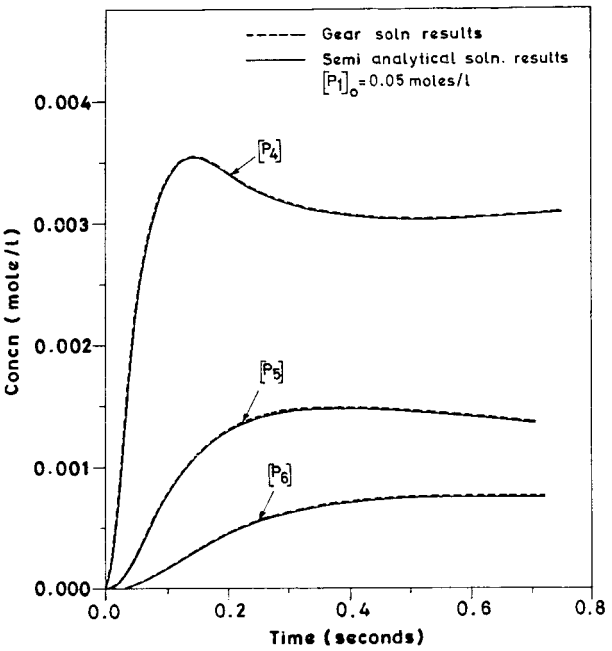

Figure 10 Comparison of results from our computation with those by Gear's technique for the first three oligomers. Concn, concentration; Soln, solution.

Now, by analogy from eq. (I.1c) and eq. (I.17), we can write

$$g_{in} = \gamma_{ni} \quad \text{(I.19)}$$

If we assume a series solution for the products of cyclization as

$$[P_1^c] = [p_{1,j-1}^c] + [M_{j-1}] \sum_{i=1}^{\infty} a1_i u^i \quad \text{(I.20a)}$$

$$[P_n^c] = [P_{n,j-1}^c] + [M_{j-1}] \sum_{i=1}^{\infty} c1n_i u^i \quad \text{for } i = 3, 4, 5, \cdots \quad \text{(I.20b)}$$

The algorithm for the coefficients of the series is given in Figure 9. The coefficients for eq. (I.20) are given in Table XI. After finding these coefficients, we test the convergence of these series using the Leibnitz convergence criterion. For the nth oligomer, $[P_n]$

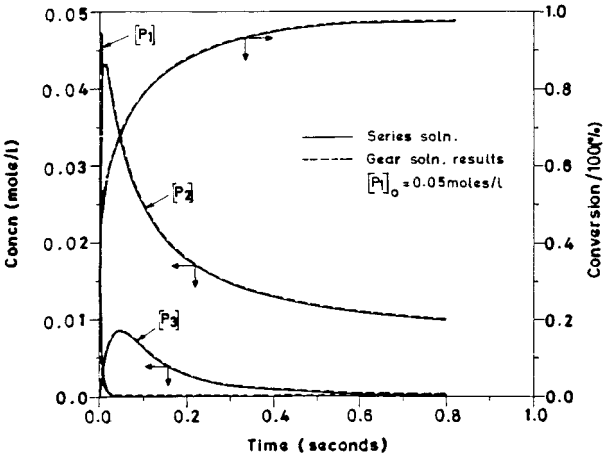

Figure 11 Comparison of results from our computation with those by Gear's technique for the higher oligomers. Concn, concentration; Soln., solution.

Table XIII Variation in Step Size with Conversion

Conversion (%)	u_t, min	u_1, min	u_2, min	u_3, min	$u_{\min}$
52.8600	0.0573	0.1078	91.560×10^{-2}	0.1616	5.730×10^{-2}
61.3560	0.0753	0.0268	2.4060×10^{-2}	0.9312	2.680×10^{-2}
70.8020	0.1950	0.0617	9.5010×10^{-2}	0.0397	3.970×10^{-2}
80.0980	0.7698	0.0197	1.8570×10^{-2}	0.7015	1.850×10^{-2}
82.1810	0.7730	0.2525	4.7100×10^{-3}	0.7322	4.710×10^{-3}
83.0122	0.7772	0.1610	1.0490×10^{-4}	0.7416	1.049×10^{-4}
83.0320	0.7773	0.1577	7.0564×10^{-7}	0.7418	7.056×10^{-7}

Initial concentrations are $[M]_0 = 0.1$ mol/L, $[P_1]_0 = 0.05$ mol/L.

$$u_{n,\min} = \min_{i=1,10} \left| \frac{\gamma_{n,i}}{\gamma_{n,i+1}} \right| \quad n = 1, 2, 3, \cdots \quad \text{(I.21)}$$

$$u_{t,\min} = \min_{i=1,10} \left| \frac{h_i}{h_{i+1}} \right| \quad \text{(I.22)}$$

Hence, the actual step size, u, for the jth step is given by

$$u_{\min} = [\min\{u_{t,\min}, u_{1,\min}, u_{2,\min}, u_{3,\min} \cdots] \quad \text{(I.23)}$$

By using the above procedure, we reach 83.9% monomer conversion in 28 iterations. After this conversion, the choice of $u_{\min}$ is found to be mainly determined by the higher oligomers and reduces to values less than 10^{-6}.

At higher conversions (>80%), we have found that the step size reduces to an order of 10^{-5}. This arises because $u_{\min}$ is governed by $[P_2]$ series. To increase the speed of computations, we have proceeded with the series solution technique and evaluated $[P_1]$, $[P_i]$, $i = 3, 4, \ldots, \infty$, and Δt but evaluated $[P_2]$ assuming that $[M]$ is constant during the iteration. For reversible anionic polymerization, the equations governing $[P_2]$, $[P_3]$, ..., $[P_n]$ are interconnected; they are solved together in the time interval Δt, with results of the previous iterations as the initial guess. If $[M]$ is assumed to be constant in this interval, the governing ODEs become linear where an analytical solution exists.[12–15] We have taken this linear estimate for $[P_2]$ instead of the series solution for $[P_2]$, while the concentrations of the other oligomers are evaluated by the series solution, as done earlier. The solution of this general mechanism of anionic polymerization thus determined has been found to be accurate and compares exceedingly well with the results of Gear's numerical technique.

Table XIV Comparison of the Series Solution Technique with the Numerical Methods

	No. of Iterations Required		
Conversion (%)	RK[a]	Gear	Series Solution
50	5,000	179	1
61	6,100	266	7
70	7,000	334	12
80	8,000	396	16
85	8,500	436	18
90	9,000	495	21
95	9,500	719	30

[a] The step size, $\Delta t = 10^{-4}$.

This algorithm was implemented on a personal computers, and in Table XII, we have varied the number of terms in the series used to compute the oligomer concentrations in eq. (I.5). In this table, we observe the effect of the increase in number of terms for the time series and also that of the first five oligomer concentrations at a monomer concentration of 0.0291 mol/L. We observe that there is a considerable difference in results using only one term from those obtained by using three terms in the series. The effect of the number of terms is more pronounced for the lower oligomers than for the higher oligomers. This may be because the concentration of the higher oligomers is quite small. The computations were carried out up to 10 terms in the series. However, there is no difference up to nine decimal places in the results computed with 5 and 10 terms. At the end of the Table XII, we have also shown the results obtained using the fourth-order Runge-Kutta method with a step size of 10^{-4}. The results are comparable (as seen in Figures 10 and 11) and are within 1% error with all computations being carried out in the double precision mode.

The step size was found by use of the Leibnitz convergence criterion with eq. (I.23). Table XIII shows the variation in step size at different monomer conversions. The $u_{n,\min}$ and $u_{t,\min}$ were computed with eqs. (I.21) and (I.22), respectively. Table XIV shows a comparison of the semianalytical technique with the standard numerical techniques. It is seen that even Gear's technique required more than 20 times the above number of iterations. Figures 10 and 11 show a comparison of the concentrations of the first six species versus time using Gear's algorithm (DO2EBF of Nag subroutine library) and semianalytical solution. The change of time with conversion has also been plotted in Figure 12. It can be seen that the curves obtained by the two technique overlap each other.

REFERENCES

1. M. Szwarc, *Carbanions, Living Polymers and Electron Transfer Processes,* Interscience Publishers, New York, 1968.
2. A. Kumar and S. K. Gupta, *Fundamentals of Polymer Science and Engineering,* Tata McGraw Hill, New Delhi, 1978.
3. G. T. Chen, *J. Polym. Sci.,* **20,** 2915 (1982).
4. M. Szwarc, *Adv. Polym. Sci.,* **49,** 1 (1983).
5. L. J. Fetters, J. Houston, R. P. Quirk, F. Vass, and R. N. Young, *Adv. Polym. Sci.,* **56,** 1 (1984).
6. A. H. E. Muller and H. Jeuck, *Makromol. Chem. Rapid Commun.,* **3,** 121 (1982).
7. C. B. Tsvetanov, A. H. E. Muller, and G. V. Schulz, *Macromolecules,* **18,** 863 (1985).
8. C. C. Chang, A. F. Halasa, and J. W. Miller Jr., *J. Appl. Polym. Sci.,* **47,** 1589 (1993).
9. R. Haswani, S. K. Gupta, and A. Kumar, *Polym. Eng. Sci.,* **35,** 1231 (1995).
10. R. R. N. Sailaja and A. Kumar, *J. Appl. Polym. Sci.,* **58,** 1865 (1995).
11. A. H. E. Muller, L. Lochmann, and J. Trekoval, *Makromol. Chem.,* **187,** 1473 (1986).
12. D. G. Schultz and J. L. Melsa, *State Functions and Linear Control Systems,* McGraw Hill, New York, 1967.
13. J. L. Melsa, *Computer Programs for Computational Assistance in the Study of Linear Control Theory,* McGraw Hill, New York, 1970.
14. M. J. Box, *Computer J.,* **8,** 1065 (1942).
15. J. L. Kuester and J. M. Maize, *Optimization Techniques with Fortran,* 1st Ed., McGraw Hill, New York, 1973.